Catalysis Letters Vol. 111, Nos. 3–4, November 2006 (© 2006)
DOI: 10.1007/s10562-006-0139-2

Silver catalysts supported over activated carbons for the selective oxidation of CO in excess hydrogen: effects of different treatments on the supports

Limin Chen, Ding Ma, Xiaoyun Li, and Xinhe Bao*

State Key Laboratory of Catalysis, Dalian Institute of Chemical Physics, Chinese Academy of Sciences, 457 Zhongshan Road, P.O. Box 110, Dalian, 116023, P.R. China

Received 8 June 2006; accepted 19 August 2006

Commercial activated carbon (AC) was used as a support either in its original form or after various modifications, giving diverse textural and surface chemical characteristics. The changes of these properties were monitored by N_2 adsorption–desorption isotherms, temperature programmed desorption (TPD) and X-ray photoelectron spectroscopy (XPS). Ag catalysts were prepared over the AC supports by a conventional wet impregnation method. The catalytic performances of supported Ag/AC catalysts in the selective oxidation of CO in excess H_2 were tested. The results indicate the textural and surface chemical characteristics are responsible for the different catalytic performances.

KEY WORDS: CO selective oxidation; activated carbon; textural properties; surface functional groups.

1. Introduction

Supported-metal catalysts are widely used in the energy-related or fine-chemical industry. It is well known that the properties of the supports have great influence on the catalytic performance. When loading active components onto/into different supports, the charges and sizes of active components [1,2], the particle shapes, the crystallographic structures [3] as well as the specific active sites at the metal-support boundary [4] can be controlled. A large volume of works have already been done on elucidating the effect of supports on the structure of metal catalysts and, subsequently, their catalytic performances [5–7]. In conclusion, the search for an appropriate support is crucial to get good supported-metal catalysts.

Carbon materials as supports have attracted growing interest due to their structural diversities and tunable surface properties [8,9]. For a specific reaction and metal precursor, it is very important to investigate the role of carbon properties (textural properties and surface functional groups) on the catalytic performance in order to find an appropriate support. The modification of textural properties was achieved by oxidation with concentrated H_2SO_4 [10] or oxidative gases (such as steam, CO_2, O_2 etc.) at high temperatures [11,12]. At the same time, oxidation in nitric acid was carried out to increase the concentration of surface functional groups; while heating under inert atmosphere can selectively remove some of these groups [13]. It was demonstrated that the modified activated carbon can be used as supports for relatively cheap Ag catalysts for selective oxidation of CO in excess hydrogen at low temperatures, which has a potential application in polymer electrolyte membrane fuel cells (PEMFCs) [14,15]. Furthermore, the electron-conductive activated carbon supported catalysts can be integrated directly into fuel cells to prevent the poison of anode Pt catalysts by CO and enhance its catalytic performance at low operating temperature (about 80 °C) [16]. Thus, it is worthy to investigate the effects of carbon properties on the catalytic performances of CO selective oxidation in excess hydrogen.

In this report, different approaches have been used to adjust the structure and surface chemistry of activated carbon and then the modified activated carbon was used as support for silver catalysts. Their performances in the selective oxidation of CO in excess hydrogen were investigated and the influences of carbon textural properties and surface chemistry are discussed.

2. Experimental

2.1. Modification of AC

Commercial granulated activated carbon (sieved into 40∼60 mesh) was obtained from Beijing Guanghua Woods Ltd. (Beijing, China). The carbon was washed with boiling aqueous nitric acid (0.001 N) and then dried at 120 °C overnight. The sample thus prepared was

*To whom correspondence should be addressed.
E-mail: xhbao@dicp.ac.cn

denoted as original AC. And, (I) AC was directly oxidized in 5 N HNO_3 solution at 80 °C for 3 h and then washed with deionized water till the pH value of the rinsed solution was above 5.0 and dried at 120 °C overnight to get AC–N. (II) The oxygen functional groups were selectively removed by heating in He at 850 °C for 30 min to obtain AC–He. (III) Steam treatment was carried out according to previous report [17] and denoted as AC–H. (IV) AC was chemically modified with concentrated H_2SO_4 at 250 °C according to literature [10] and then heated in He at 850 °C for 30 min, the sample thus obtained was labeled as AC–S–He.

2.2. Characterization

The texture properties of carbon supports were determined by N_2 adsorption–desorption isotherms at 77 K using an AS-1-MP adsorption instrument. Samples were degassed at 383 K overnight before the measurements [18]. The specific surface areas were calculated using the BET equation, and the t-plot method was used to calculate the micropore volumes and areas [10]. The total pore volumes were estimated to be the liquid N_2 volumes at relative pressure of 0.98. The values of mesopore volumes and areas were obtained by subtracting the micropore volumes and areas from the total volumes and BET areas, respectively.

The TPD experiments were carried out in a quartz U-type microreactor, connected with an on-line quadruple mass spectrometer (Balzers, OmniStar GSD300 O). The samples (0.1 g) were first flushed with He (30 ml/min) at room temperature for 2 h. Subsequently, the temperature was increased to 990 °C at the rate of 5 °C/min. MS intensities for 2 (H_2), 4 (He), 28 (CO), and 44 (CO_2) were measured as a function of temperature.

XPS measurements were performed on an Amicus XPS spectrometer using non-monochromatic MgKα radiation (1253.6 eV). The C 1s binding energy (BE) of the graphitic carbon (284.6 eV) was used as reference [19,20]. Prior to individual elemental scans, a survey scan was taken for all of the samples in order to estimate the elements present. In this work, only carbon and oxygen have been detected, and the corresponding elemental composition was calculated from XPS spectra after correcting the peak areas by sensitivity factors.

Transmission electron microscopy (TEM, JEOL JEM-2000EX) was used to observe the size of silver particles.

2.3. Catalyst preparation

AC and all modified AC were used as supports to prepare 12 wt% Ag catalysts by a conventional wet impregnation method using aqueous silver nitrate ($AgNO_3$, Shanghai Chemical Reagent Company, 99.9%). The as-prepared catalysts were dried at 120 °C for 12 h and then treated under H_2 at 500 °C for 2 h before catalytic tests.

2.4. Catalytic reaction test

The catalytic reaction tests were performed in a fixed-bed flow reactor. A gas mixture containing 1% CO and 0.5% O_2 (volume ratio) in H_2 was fed at a flow rate of 50 ml/min. The composition of the effluent gas was monitored on-line with a gas chromatograph (Agilent Technologies GC-6890N) equipped with PN and TDX-01 columns. The CO conversion was calculated from the change in CO concentration, and selectivity towards CO_2 was calculated from the O_2 mass balance. The details were reported previously [21].

3. Results and discussion

3.1. Textural properties of supports

Table 1 shows the textural properties of all AC supports. It is concluded that nitric acid oxidation and heating under He (AC–N and AC–He versus AC) treatments have little impact on the texture of AC, while heating under He after treating with concentrated H_2SO_4 (AC–S–He) and steam treatment at high temperature (AC–H) alter the textural properties of AC significantly. Both methods have almost doubled mesoporous surface areas as compared with that of native AC or AC–He, and the volumes corresponding to mesopores were significantly increased and so did the total surface areas. On top of that, in the case of AC–H, large amount of micropores were created upon steam treatment, which agrees well with previous reports [10–13].

3.2. Surface functional groups of supports

3.2.1. TPD results

Temperature-programmed desorption experiments using an inner gas (He, Ar, N_2) are effective in determining different oxygen-containing groups of carbon materials [22–24]. Figure 1 shows the TPD profiles of the AC before and after different treatments. An increase of surface functional groups after oxidation with aqueous nitric acid (AC–N) is obvious as evidenced by the increase of CO (figure 1a) and CO_2 (figure 1b)

Table 1
The textural properties of AC before and after modification

Sample	S_{BET} (m^2/g)	S_{micro} (m^2/g)	S_{meso} (m^2/g)	V_{total} (cm^3/g)	V_{meso} (cm^3/g)
AC	1058	831	227	0.54	0.28
AC–N	1043	828	215	0.52	0.27
AC–He	1051	793	258	0.51	0.26
AC–S–He	1197	797	400	0.57	0.33
AC–H	1423	1031	392	0.76	0.43

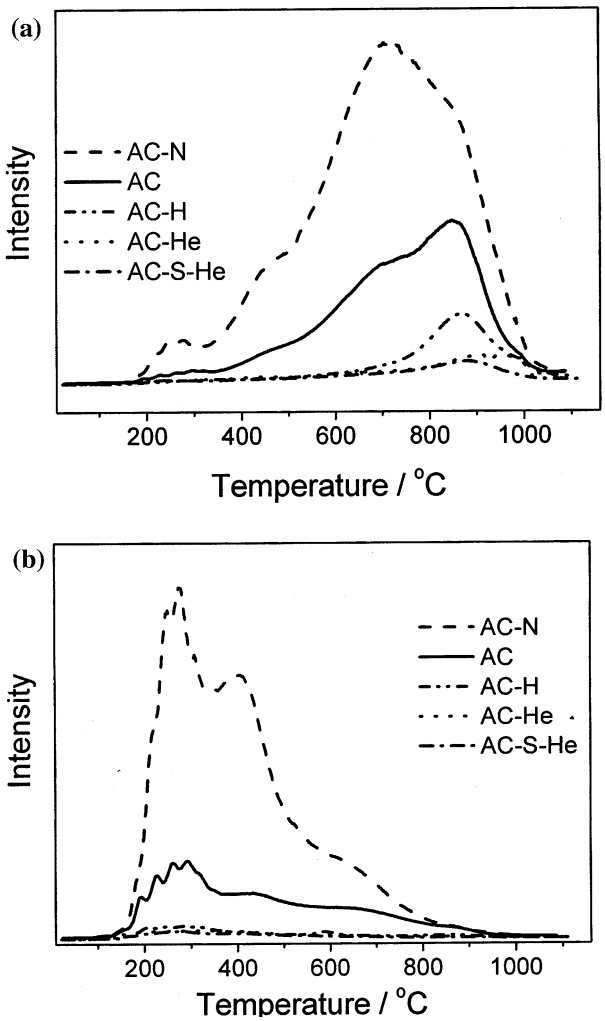

Figure 1. The profiles of CO (a) and CO_2 (b) evolution of AC after different treatments in TPD experiments.

intensities. AC–He and AC–S–He released very small amount of CO (figure 1a) and CO_2 (figure 1b) compared with native AC. This indicates that most surface functional groups have been removed after the He treatment. Similarly, treating AC with steam at 850 °C killed most surface functional groups and only small amount of CO release was observed.

According to literature [22–24], acidic carboxylic and lactol (also lactone) groups, release CO_2 at about 270 °C and 380–670 °C, respectively, in the TPD experiments, while carboxylic anhydride groups decompose with simultaneous formation of CO and CO_2 at 430–570 °C (as shown in figure 1). Less acidic Phenol and carbonyl/quinone groups are more stable on the carbon surface and decompose to CO at about 630 and 850 °C, respectively (as shown in figure 1a). Thus, it can be concluded that AC–N has more acidic and less acidic groups, AC has much less functional groups while AC–He, AC–S–He and AC–H have very limited amount of less acidic functional groups.

3.2.2. XPS results

TPD measurements can determine oxygen-containing groups on carbon materials, while XPS analysis can provide information about the surface composition. The surface compositions of carbon supports from XPS analysis are shown in table 2. For AC–N, AC, and AC–He, the surface concentration of oxygen atomic are 17.7%, 11.8%, and 7.4%, respectively; and the corresponding O/C value is 0.215, 0.134, and 0.080, respectively. These data demonstrated that oxygen content has been increased after oxidation in nitric acid (AC–N versus AC), while treatment in He at high temperature will remove the oxygen-containing groups (AC–He versus AC). Similarly to AC–He, most oxygen-containing groups have been killed after treating with steam (AC–H) or concentrated sulfuric acid oxidation followed with high temperature He treatment (AC–S–He). Thus, for AC–He, AC–S–He and AC–H, the oxygen content and O/C value are very close to each other, i.e., around 7.5% and 0.085, respectively. These surface compositions from XPS analysis are in good agreement with TPD results that AC–N contains the highest amount of oxygen functional groups, and AC has much less functional groups while AC–He, AC–S–He and AC–H have very limited amount of functional groups.

3.3. Reaction results

Figure 2 presents the highest CO conversion and the corresponding oxygen selectivity towards CO_2 over various 12 wt% Ag/AC catalysts (the reaction temperature for individual catalyst is also marked). All catalysts reached the full or near full oxygen conversion at the point of maximum CO conversion. Among three catalysts, i.e., Ag/AC–N, Ag/AC and Ag/AC–He, Ag/AC–He shows the highest maximum CO conversion (23.2%) at higher reaction temperature (80 °C); however, Ag/AC–N catalyst presents the lowest maximum CO conversion (18.4%) at much lower reaction temperature (62 °C). In the group of Ag/AC–He, Ag/AC–S–He and Ag/AC–H catalysts, the maximum CO conversion over Ag/AC–S–He (26.8%, 78 °C) is apparently higher than that of Ag/AC–He (23.2%, 80 °C) and Ag/AC–H catalyst (16.7%, 86 °C).

Different catalysts give maximum CO conversion at different temperatures with nearly full oxygen conversion

Table 2
Surface composition of carbon supports by XPS analysis

Sample	C (at.%)	O (at.%)	O/C atomic ratio
AC–N	82.3	17.7	0.215
AC	88.2	11.8	0.134
AC–He	92.6	7.4	0.080
AC–S–He	92.1	7.9	0.086
AC–H	92.0	8.0	0.087

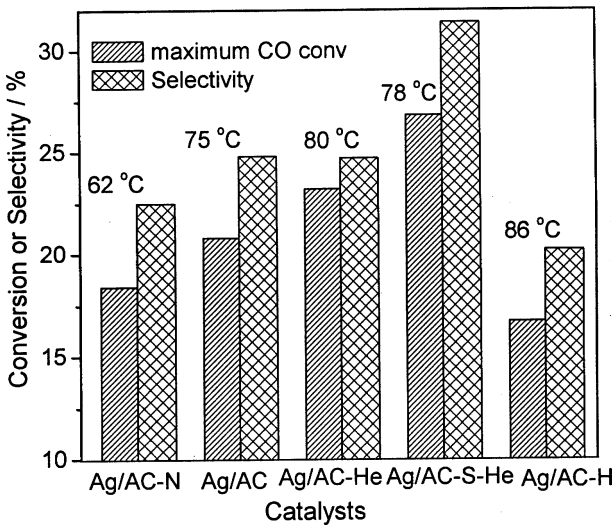

Figure 2. The highest CO conversion and the corresponding selectivity towards CO_2 over various 12 wt% Ag/AC catalysts.

which indicates different catalysts have different catalytic activities even at the same reaction temperature. Figure 3 presented O_2 and CO conversion at 62 °C over various 12 wt% Ag/AC catalysts. As shown, Ag/AC–N gives 100% oxygen conversion with 18.4% CO conversion. Instead, much lower oxygen conversion was detected (about 50%) with 15.6% CO conversion over Ag/AC catalyst. Again, even lower oxygen conversion was observed over Ag/AC–He catalyst, close to 45% with 17.0% CO conversion. Ag/AC–S–He catalyst presented lower O_2 conversion (42.5%) but with higher CO conversion (about 20%) compared with Ag/AC–He catalyst. The lowest O_2 and CO conversion (27.3% and 8.6%, respectively) was obtained over Ag/AC–H catalyst.

From these reaction data, it is concluded that Ag/AC–N catalyst shows highest catalytic activity toward oxygen consumption and CO oxidation among Ag/AC–N, Ag/AC and Ag/AC–He catalysts, while Ag/AC–S–He catalyst presents highest CO oxidation catalytic activity with moderate oxygen consumption activity among Ag/AC–He, Ag/AC–S–He and Ag/AC–H catalysts. Ag/AC–H catalyst has the lowest catalytic activity toward oxygen consumption and CO oxidation among all catalysts.

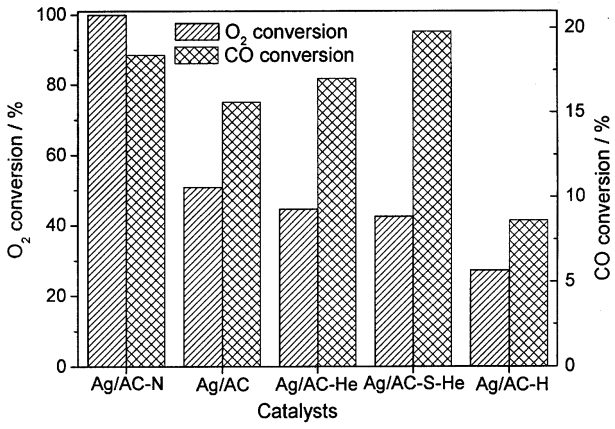

Figure 3. The O_2 and CO conversion at 62 °C over various 12 wt% Ag/AC catalysts after activation in H_2 at 500 °C for 2 h.

3.4. Discussion

Generally, suitable surface functional groups, high specific surface area and well developed porosity of the carbon supports are essential for achieving better metal dispersion, which usually has direct relationship with catalytic performance (proper metal particle sizes are necessary for some specific reactions though). However, it is difficult to differentiate the impact of those factors on the catalytic performances as different supports in most cases are different in all those aspects. However, herein, AC–He, AC–S–He and AC–H supports have similar amounts of surface functional groups according to TPD and XPS results, but with different porosities. Therefore, the difference of the catalytic performances can only be ascribed to their different porosities, and to thus resulted different metal particle sizes. AC–S–He has larger mesopore area compared with AC–He. After impregnated with silver, small Ag particles (most of them are around 10–12 nm, figures 4d and 5d) was observed over Ag/AC–S–He catalyst, compared with that of Ag/AC–He (around 12 nm, but with a much more diverse size distribution; figures 4c and 5c). In the case of Ag/AC–H, large Ag particles dominate the TEM picture (about 18–30 nm, figures 4e and 5e), compared with Ag/AC–S–He catalyst, which indicates that the existence of large amount of micropores may play a negative role in the dispersion of metal particles.

It is observed that the properties of the catalysts are not merely a function of the porosity, but more of the support surface chemistry. For AC–N, AC and AC–He supports, they are similar in terms of the textural properties, thus the difference of the catalytic performance can only be attributed to their surface functional groups-induced different silver particle size distribution. Those surface functional groups can lead to the reduction of Ag^+ during the impregnation process, followed by the heterogeneous and/or homogeneous nucleation during activation process, thus the metal particle size distribution are found to be bimodal [7,15], especially for carbon supports with rich functional groups (TPD and XPS data). At the same time, functional groups can increase the dispersion of particles, and promote the formation of very fine silver nanoparticles (around 2–6 nm, see figures 4a and 5a).

Usually, the amount of acidic groups (evolving as CO_2 upon TPD at relatively low temperature) is significantly increased for AC after oxidation with nitric acid (AC–N), and correspondingly the hydrophobicity of the carbon decreases [25], making its surface more accessible for the silver species in the aqueous phase during the

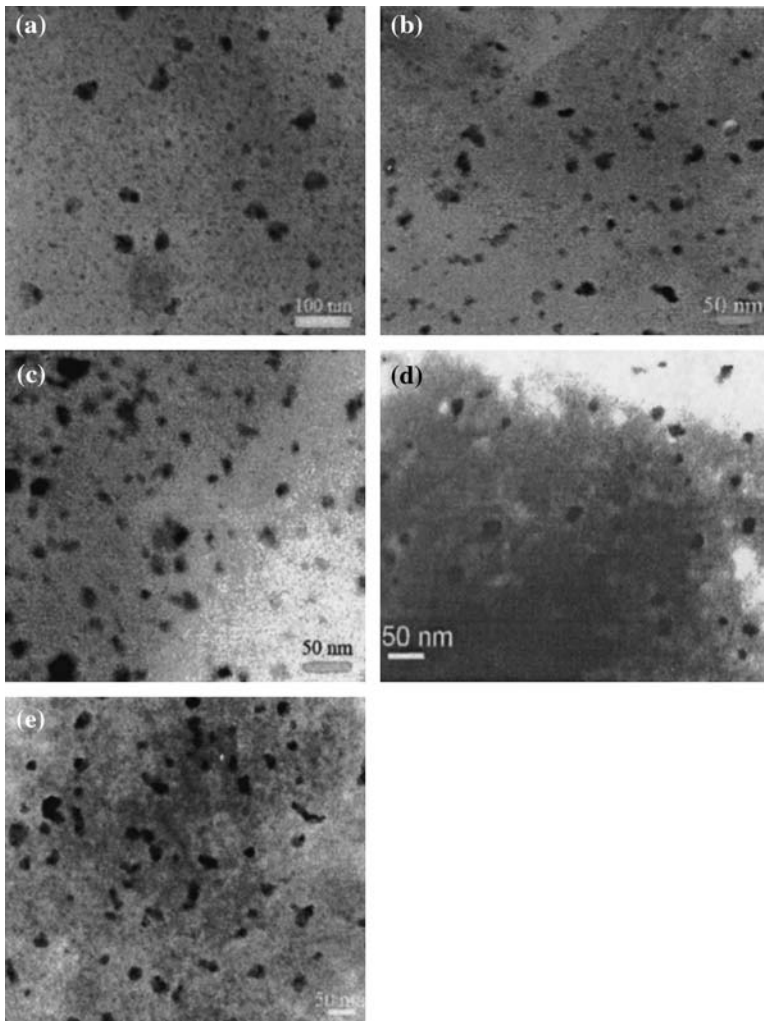

Figure 4. TEM pictures of various 12 wt% Ag/AC after activation in H_2 at 500 °C for 2 h: (a) Ag/AC–N, (b) Ag/AC, (c) Ag/AC–He, (d) Ag/AC–S–He, (e) Ag/AC–H.

impregnation process. However, for AC after heating under He, large amount of acidic groups were removed which resulted in the increased hydrophobicity of the carbon. Furthermore, oxidation with nitric acid (AC–N) also significantly increased the amount of less acidic oxygen groups (evolving as CO at high temperature in TPD experiments) which promoted the interaction of the Ag precursor/Ag particles with the supports [7], and as a consequence, prevented the sintering of those Ag particles. In addition, the carbon surface may have different amounts and types of surface functional groups and consequently it can be negatively and positively charged in aqueous solution, depending on the pH value. At certain pH values (the isoelectric point, pH_{IEP}), the overall surface charge will be zero. Here, the pH_{IEP} of the supports follows the order of: pH_{IEP} (AC–N) < pH_{IEP} (AC) < 7 < pH_{IEP} (AC–He). The pH value of aqueous $AgNO_3$ is close to seven, so, the supports, AC–N and AC, having pH > pH_{IEP} (AC–N or AC) and being covered by deprotonated carboxyl groups, have strong interaction with Ag^+ from solution; instead, for the AC–He, where pH < pH_{IEP} (AC–He), attraction of anions will be preferred [5].

The effects of surface functional groups are very complicated during the catalyst preparations and the final silver particle size is determined by all factors mentioned above. In the case of the Ag/AC–N catalyst, the silver particles present bimodal distribution apparently; the size of small ones is about 2–6 nm, while the big ones are larger than 22 nm, as shown in figures 4a and 5a. On the contrary, the particle of Ag/AC–He catalyst has a wider distribution with a peak at 12 nm (figures 4c and 5c). For Ag/AC catalyst, the size is centered at 6–8 nm (as shown in figures 4b and 5b).

The particle size has good correlation with the catalytic activity, i.e., the smaller the Ag particle size, the higher the activity (which can be defined as the temperature for full oxygen conversion or the oxygen conversion at the same reaction temperature). In the case of Ag/AC–N, the full oxygen conversion was reached at 62 °C

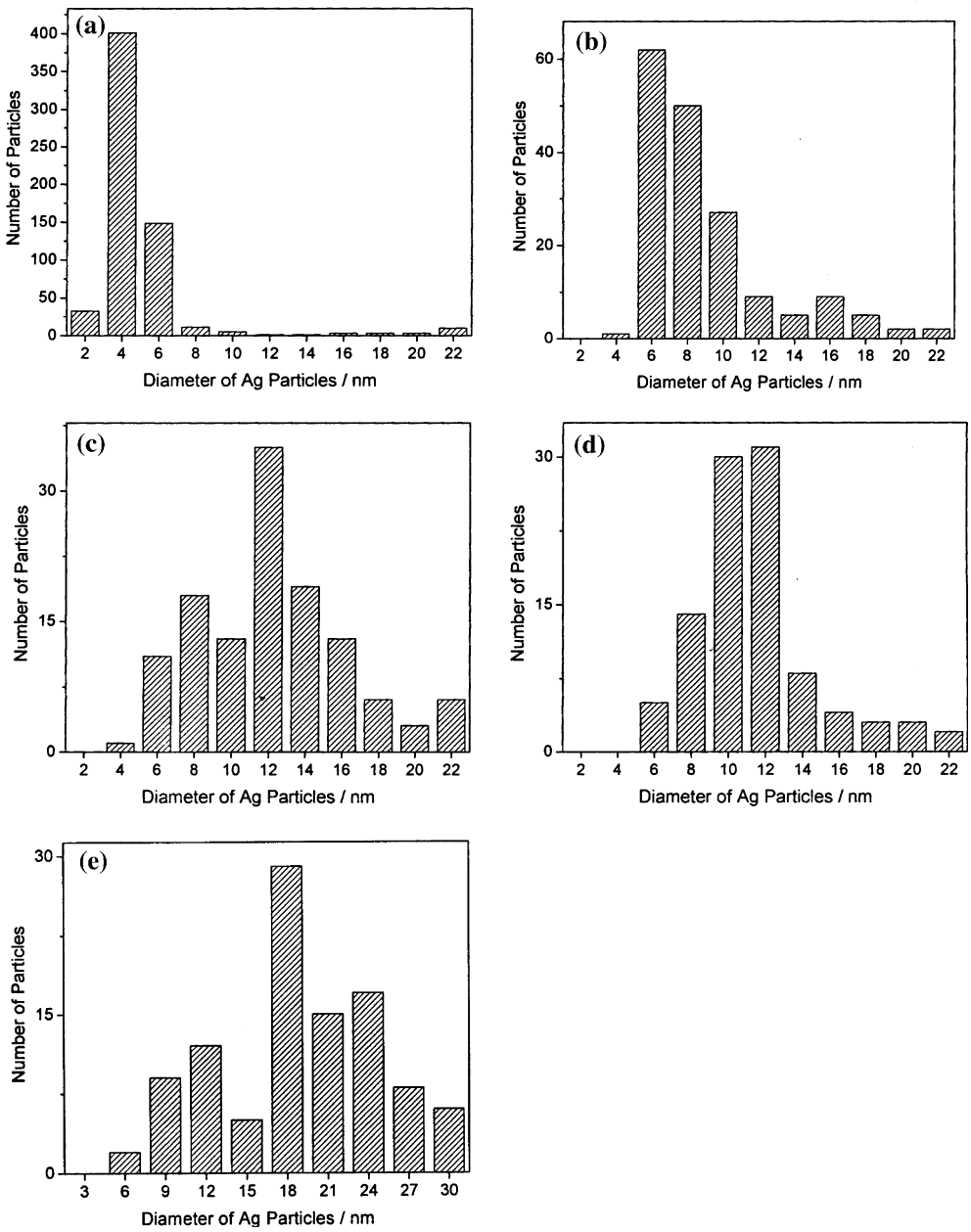

Figure 5. Size distribution of Ag particles for various 12 wt% Ag/AC after activation in H_2 at 500 °C for 2 h: (a) Ag/AC–N, (b) Ag/AC, (c) Ag/AC–He, (d) Ag/AC–S–He, (e) Ag/AC–H. For (a)–(d), the number of particles larger than 22 nm has been combined.

while that of the other four catalysts is higher than 75 °C. However, the smaller particles would also benefit the combustion of hydrogen, which leads to a lower maximum CO conversion, especially in the case of Ag/AC–N catalyst. Increasing Ag particle size resulted in the lower catalytic activity but higher maximum CO conversion (Ag/AC, Ag/AC–He and Ag/AC–S–He catalysts). As the size of Ag particles increased further (Ag/AC–H), both catalytic activity and maximum CO conversion decreased. However, there is proper Ag particle sizes for CO oxidation (around 10–12 nm, Ag/AC–S–He) which confirms our previous observation [26].

4. Conclusions

Both textural properties and surface functional groups of carbon supports have great impact on CO selective oxidation in excess H_2. Large amounts of mesopore tend to increase the dispersions of Ag particles, thus, giving higher maximum CO conversion at low temperature; instead, negative effect of microporous structure on the dispersions of Ag particles and catalytic performance maybe has been observed. Rich surface functional groups on one hand make size distribution of Ag particles bimodal, but on the other hand promote

the formation of very fine Ag particles, leading to low maximum CO conversion at low temperature. A proper silver particle size is essential for the good catalytic performance.

Acknowledgments

This work was supported by the Chinese Ministry of Science and Technology (2003CB6 15806) and the Natural Science Foundation of China (National Key Project: 90206036).

References

[1] S.J. Miao, Y. Wang, D. Ma, Q.J. Zhu, S.T. Zhou, L.L. Su, D.L. Tan and X.H. Bao, J. Phys. Chem. B 108 (2004) 17866.
[2] Z.P. Qu, W.X. Huang, S.T. Zhou, H. Zheng, X.M. Liu, M.J. Cheng and X.H. Bao, J. Catal. 234 (2005) 33.
[3] M. Vaarkamp, J.T. Miller, F.S. Modica and D.C. Koningsberger, J. Catal. 163 (1996) 294.
[4] P.V. Menacherry, M. Fernandez-Garcia and G.L. Haller, J. Catal. 166 (1997) 75.
[5] F. Rodriguez-Reinoso, Carbon 36 (1998) 159.
[6] E.D. Park and J.S. Lee, J. Catal. 193 (2000) 5.
[7] D.A. Bulushev, I. Yuranov, E.I. Suvorova, P.A. Buffat and L. Kiwi-Minsker, J. Catal. 224 (2004) 8.
[8] Ph. Serp, M. Corrias and Ph. Kalck, Appl. Catal. A 253 (2003) 337.
[9] E. Auer, A. Freund, J. Pietsch and T. Tacke, Appl. Catal. A 173 (1998) 259.
[10] Z.X. Jiang, Y. Liu, X.P. Sun, F.P. Tian, F.X. Sun, C.H. Liang, W.S. You, C.R. Han and C. Li, Langmuir 19 (2003) 731.
[11] H. Teng, Y.T. Tu, Y.C. Lai and C.C. Lin, Carbon 39 (2001) 575.
[12] E. Aksoylu, M.M.A. Freitas, M.F.R. Pereira and J.L. Figueiredo, Carbon 39 (2001) 175.
[13] J.L. Figueiredo, M.F.R. Pereira, M.M.A. Freitas and J.J.M. Órfão, Carbon 37 (1999) 1379.
[14] H. Igarashi, T. Fujino and M. Watanabe, J. Electroanal. Chem. 391 (1995) 119.
[15] L.M. Chen, D. Ma, B. Pietruszka and X.H. Bao, J. Nat. Gas Chem. (in press).
[16] H.M. Yu, Z.J. Hou, B.L. Yi and Z.Y. Lin, J. Power Sources 105 (2002) 52.
[17] Z.X. Jiang, Y. Liu, X.P. Sun, Z.Q. Shen, C.R. Han and C. Li, Chinese J. Catal. 24 (2003) 649.
[18] F. Rodriguez-Reinoso, J.M. Martin-Martinez, C. Prado-Burguete and B.A. McEnaney, J. Phys. Chem. 91 (1987) 515.
[19] E. Desimoni, G.I. Casella, A. Morone and A.M. Salvi, Surf. Interface Anal. 15 (1990) 627.
[20] H. Estrade-Szwarckopf, Carbon 42 (2004) 1713.
[21] Z.P. Qu, M.J. Cheng, X.L. Dong and X.H. Bao, Catal. Today 93–95 (2004) 247.
[22] S. Haydar, C. Moreno-Castilla, M.A. Ferro-Garcia, F. Carrasco-Marin, J. Rivera-Utrilla, A. Perrard and J.P. Joly, Carbon 38 (2000) 1297.
[23] U. Zielke, K.J. Huttinger and W.P. Hoffman, Carbon 34 (1996) 983.
[24] Y.F. Jia and K.M. Thomas, Langmuir 16 (2000) 1114.
[25] C. Prado-Burguete, A. Linares-Solano, F. Rodriguez-Reinoso and C. Salians-Martinez De Lecea, J. Catal. 128 (1991) 397.
[26] Z.P. Qu, M.J. Cheng, W.X. Huang and X.H. Bao, J. Catal. 229 (2005) 446.